

Valence Band Structure Engineering in Graphene Derivatives

Vladimir V. Shnitov, Maxim K. Rabchinskii, Maria Brzhezinskaya,* Dina Yu. Stolyarova, Sergey V. Pavlov, Marina V. Baidakova, Aleksandr V. Shvidchenko, Vitaliy A. Kislenko, Sergey A. Kislenko, and Pavel N. Brunkov

Engineering of the 2D materials' electronic structure is at the forefront of nanomaterials research nowadays, giving an advance in the development of next-generation photonic devices, e-sensing technologies, and smart materials. Herein, employing core-level spectroscopy methods combined with density functional theory (DFT) modeling, the modification of the graphenes' valence band (VB) upon its derivatization by carboxyls and ketones is revealed. The appearance of a set of localized states in the VB of graphene related to molecular orbitals of the introduced functionalities is signified both experimentally and theoretically. Applying the DFT calculations of the density of states projected on the functional groups, their contributions to the VB structure are decomposed. An empirical approach, allowing one to analyze and predict the impact of a certain functional group on the graphenes' electronic structure in terms of examination of the model molecules, mimicking the introduced functionality, is proposed and validated. The interpretation of the arising states origin is made and their designation, pointing out their symmetry type, is proposed. Taken together, these results guide the band structure engineering of graphene derivatives and give a hint on the mechanisms underlying the alteration of the VB structure of 2D materials upon their derivatization.

1. Introduction

Band structure engineering of the 2D materials via the formation of 2D Moiré heterostructures,^[1,2] structural patterning,^[3,4] or chemical derivatization is a subject of significant attention in the nanomaterials research community nowadays.^[5–7] Major efforts are being focused on the controllable tuning of the band gap, the density of states (DOS) in the valence, and conduction bands of elemental 2D materials, such as borophene, silicene, etc.,^[4] hexagonal boron nitride and molybdenum disulfide,^[5,6] and, especially, graphene, owing to advances in its manufacturing and derivatization.^[7–9] As a result, a large family of Moiré materials and derivatives of 2D materials with the engineered electronic structure has emerged and found its application in the next-generation photonics, optoelectronics, and sensing devices as well as the development of smart materials.^[10–12]

Despite these achievements upon almost two decades of extensive studies, the puzzling interplay between the structure, chemistry, and band structure of 2D materials still remains a fundamental bottleneck, hindering the further advances in the tuning of their physics. Regarding the chemical derivatization of graphene as one of the most facile and thoroughly studied ways to adjust the band structure,^[8,9] non-stoichiometric, dynamic chemical composition, and spatial arrangement of the modifying organic groups obscure their influence on the DOS of the synthesized chemically modified graphenes (CMGs).^[13,14] Both experimental and theoretical investigations are being carried out to reveal the effect of graphene derivatization by oxygen, fluorine, or hydrogen moieties as well as doping with various elements on the alteration of graphene's band gap, the introduction of the molecular-related states, and DOS modification near the Fermi level.^[9,15–22] Main results were achieved within the frame of the studies on the graphene oxide (GO) and fluorographene, namely oxidized and fluorinated counterparts of graphene,^[8,9] which have shown that depending on the concentration of the oxygen or fluorine groups on the graphene basal plane the band gap can be tuned within the range of 0.11–3 eV.^[16,19,21] In turn, the rise of a band gap from 0 to 0.60 eV by doping graphene with nitrogen or boron was reported owing to the alteration of both the Fermi level position and density of π states near it by the embedded atoms.^[23,24]

V. V. Shnitov, M. K. Rabchinskii, M. V. Baidakova, A. V. Shvidchenko, P. N. Brunkov
Ioffe Institute
Politekhnikeskaya St. 26, Saint Petersburg 194021, Russia


M. Brzhezinskaya
Helmholtz-Zentrum Berlin für Materialien und Energie
Hahn-Meitner-Platz 1, 14109 Berlin, Germany
E-mail: maria.brzhezinskaya@helmholtz-berlin.de

D. Y. Stolyarova
NRC “Kurchatov Institute”
Akademika Kurchatova pl. 1, Moscow 123182, Russia

S. V. Pavlov, V. A. Kislenko
Center for Computational and Data-Intensive Science and Engineering
Skolkovo Institute of Science and Technology
Skolkovo Innovation Center, Nobel St. 3, Moscow 143026, Russia

S. V. Pavlov, V. A. Kislenko, S. A. Kislenko
Joint Institute for High Temperatures of RAS
13/2 Izhorskaya St., Moscow 125412, Russia

S. A. Kislenko
Moscow Institute of Physics and Technology
9 Institutskiy per., Dolgoprudny 141701, Russia

 The ORCID identification number(s) for the author(s) of this article can be found under <https://doi.org/10.1002/smll.202104316>.

© 2021 The Authors. Small published by Wiley-VCH GmbH. This is an open access article under the terms of the Creative Commons Attribution License, which permits use, distribution and reproduction in any medium, provided the original work is properly cited.

DOI: 10.1002/smll.202104316

However, the origin and evolution of electronic states in the valence band (VB) of CMGs away from the Fermi level, in the range of binding energy (BE) of ca. 3.5–30 eV remains poorly studied. Few publications devoted to the experimental examination of the VB structure of GO and reduced GO (rGO) compared to the highly oriented pyrolytic graphite can be found.^[17,25,26] Apart from the GO and rGO, only aminated graphene was reported to be investigated experimentally in terms of the modification of VB spectra upon the functionalization.^[27] In all cases, besides the identification and detailed analysis of the π and σ -related states of graphene lattice, thanks to the well-known electronic structure of graphene and graphite, only generalized interpretation of the oxygen-related states has been given.^[22,24,25] The appearance of additional electronic states and DOS modification upon the introduction of a certain oxygen group (carboxyl, ketone, hydroxyl, etc.) is still not well understood. At the same time, given these findings, strategies for the synthesis of CMGs, their use for the Moiré materials formation, and subsequent applications can be developed.

Herein, we employed core-level spectroscopy methods combined with density functional theory (DFT) modeling to track the modification of VB spectra of graphene upon its functionalization by certain oxygen groups. A set of graphene derivatives, from conventional GO and rGO layers to carbonylated (C-ny) and carboxylated (C-xy) graphenes predominantly functionalized by ketones and carboxyl groups, respectively,^[28,29] were examined. Synthesized by means of wet-chemistry selective reduction and photochemical modification of GO and possessing holey structure, C-ny and C-xy graphene contain up to 9 at% of ketones and carboxyl groups, respectively, with a minor content of other oxygen groups. Taking advantage from this fact, we unveiled the nature of VB states in graphene derivatives, which originate from the impact of molecular orbitals (MOs) of carboxyl groups and ketones modifying the edges of the graphene network. A facile empirical approach for the determination of the molecular-related states in the DOS of the functionalized

graphene by comparative analysis with the model organic molecules is proposed and validated. The origin of each molecular state in the ketones and carboxyl groups is revealed by the theoretical calculations of both the DOS of the whole CMG layer and its projection solely on the modifying group. Based on the revealed similarity of molecular-related states in the CMGs and model molecules, the nomenclature for the notation of these states, pointing out their symmetry type, is proposed. As a net result, these results make an advance in the field of the band structure engineering of graphene derivatives, their use for Moiré structures formation as well as give a hint on the fundamental mechanisms underlying the alteration of the VB structure of 2D materials upon their chemical derivatization.

2. Results and Discussion

Figure 1a displays high-resolution C 1s core-level X-ray photoelectron spectra (XPS) of C-ny graphene, C-xy graphene, GO, and rGO. Six components of different origin are discerned in the C 1s spectra of C-ny graphene, C-xy graphene, and GO, whereas the rGO spectrum is presented by a single C=C peak with binding energy (BE) of 284.6 eV, corresponding to carbon atoms of pristine or weakly distorted π -conjugated graphene network (sp^2 -domains).^[27,30] The asymmetry of this spectral feature originates from the intense generation of electron–hole ($e-h$) pairs produced by escaping photoelectrons.^[31,32] In the case of GO, the low extent of π -conjugation suppresses this process and the asymmetry of the C=C peak is diminished. Note that commonly two additional spectral features, C–V peak and C–C peak with BEs of 283.8 and 285.1 eV, respectively, are distinguished in the C 1s spectra of graphenes and carbon nanotubes.^[33,34] Related to the carbon atoms adjacent to the ones covalently bonded to modifying groups and unterminated carbon atoms at the edges of vacancies, respectively,^[33] in our case these peaks comprise the C=C peak.

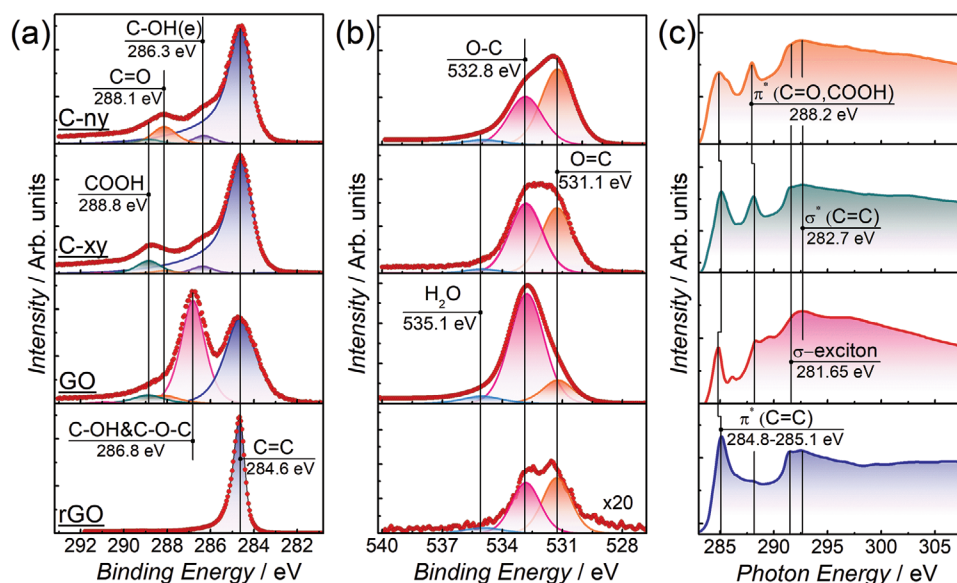


Figure 1. Chemistry of graphene derivatives examined by means of core-level techniques. a) C 1s and b) O 1s core-level X-ray photoelectron spectra of C-ny graphene, C-xy graphene, GO, and rGO. c) C K-edge X-ray absorption spectra of the graphene derivatives.

The rest of the components are related to the carbon atoms of the graphene network functionalized by various oxygen groups. The hydroxyls and epoxides located on the basal plane of graphene layers reveal themselves by the C–OH&C–O–C peak with a BE of 286.8 eV,^[30] which is the envelope of two components, referring to hydroxyls and epoxides.^[35] However, due to their proximity, they cannot confidently be distinguished and the changes in the relative concentration of hydroxyls and epoxides are manifested only by a shift in the peaks' from BE = 286.8 eV to BE = 286.5 eV. In turn, the components with BE of 286.3, 288.1, and 288.8 eV refer to the retained edge-located hydroxyl or ether moieties (C–OH(e) peak), ketones (C=O peak), and carboxyls (COOH peak), respectively.^[29,30,33] The presence of the two latter oxygen groups is also indicated in the O 1s spectra by a prominent O=C peak with BE of 531.2 eV (Figure 1b), which refers to the oxygen atoms that participate in double carbon–oxygen bonds.^[30] At the same time, hydroxyls and epoxides with single carbon–oxygen bonds give rise to a component with BE = 532.8 eV (peak O–C). The third component, the H₂O peak with BE = 535.1 eV is attributed to the presence of the molecules of interlayer water.^[30,36]

The predominant functionalization of C-ny graphene and C-xy graphene by ketones and carboxyl groups upon the GO derivatization is also pointed out by the evolution of the C K-edge X-ray absorption spectra (XAS) displayed in Figure 1c. The peak π^* (C=O, COOH) centered at $h\nu = 288.2$ eV, corresponding to electron transitions from the core levels to π^* orbitals localized on ketones and carboxyl groups, becomes well-defined and dominant along with the π^* resonance of the conjugated C=C bonds at $h\nu = 284.8$ – 285.1 eV.^[30,37] In the initial GO this π^* resonance is hardly discerned, while it is completely absent in the case of rGO.

Fourier transformed infrared (FTIR) spectra further supports the core-level spectroscopies data. Figure 2a shows the IR spectra of the pristine GO, rGO, C-ny graphene, and C-xy

graphene. Upon the conversion of GO into C-ny graphene or C-xy graphene, most of the absorption bands associated with different oxygen-containing functionalities initially presented in the GO disappear or diminish. The broad absorption band at $\nu = 2900$ – 3700 cm^{-1} , corresponding to the stretching and bending vibrations of the O–H bonds of the molecules of interlayer water, hydroxyl, and carboxyl groups,^[38] vanishes. Spectral bands at $\nu = 1365$ – 1415 , $\nu = 1220$, and $\nu = 972$ cm^{-1} related to the basal-plane hydroxyls, epoxides, and lactols almost disappear.^[38,39] At the same time, the characteristic absorption band of C=O vibrational modes of ketones and carboxyls centered at $\nu \approx 1720$ cm^{-1} demonstrates almost no diminishing or even rises in the case of C-xy graphene. This verifies the abundance of edge-modifying carbonyl and carboxyl moieties in the C-ny graphene and C-xy graphene.

Besides, the absorption band at $\nu = 1060$ cm^{-1} commonly attributed to edge-located hydroxyls is retained to some extent,^[38,40] which coincides with the XPS data. In the case of C-ny graphene, the presence of the intensive and broadened band at $\nu = 1220$ cm^{-1} is indicated although the XPS data signify the elimination of epoxides, which is suggested to be related to the formation of the in-plane ethers along with ketones.^[41] Moreover, the new absorption feature at $\nu = 1580$ cm^{-1} arises that belongs to vibrations of the C=C bonds in the localized domains of the pristine graphene network. This absorption band reduces upon moving to C-xy graphene and further to rGO due to merging of the initially isolated sp^2 -domains and raising of the overall delocalization rate of the system of π -bonds, which results in the broadening and subsequent vanishing of the corresponding IR absorption band. Alteration in the extent of the π -conjugated areas of the graphene network is also indicated by the XAS data. In C-xy graphene alike as in rGO, π^* resonance of the conjugated C=C bonds is narrow and intensive, which in combination with the appearance of the discernable σ^* -exciton positioned at $h\nu = 291.65$ eV implies nearly

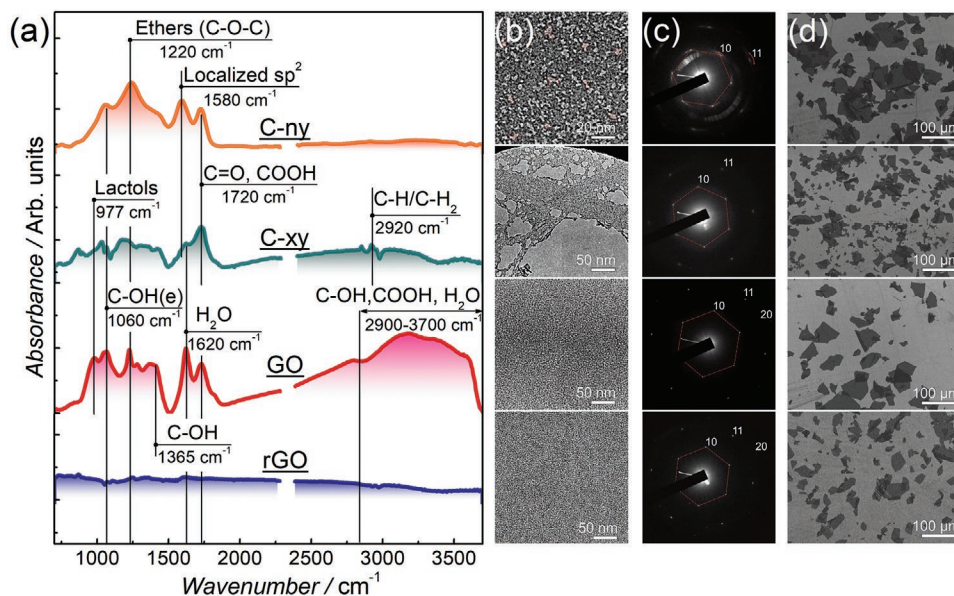


Figure 2. Chemistry and morphology of graphene derivatives. a) FTIR spectra, b) transmission electron microscopy (TEM) images, c) electron diffraction (ED) patterns, and d) scanning electron microscopy (SEM) C-ny graphene, C-xy graphene, GO, and rGO.

complete recuperation of the extended conjugated domains of the graphene network.^[42] Oppositely, in the spectrum of C-ny graphene C=C π^* resonance is broadened and has a lower intensity in comparison to the σ^* resonance at $h\nu = 282.7$ eV, which mature from the C=C bonds of the small localized sp^2 -domains of varied dimensions having a diverse conjugation length.

Difference in the degree of π -conjugation in C-ny graphene, C-xy graphene, and rGO arises from the perforation of the graphene layer which inevitably accompanies by the introduction of a high number of ketones and carboxyl groups. This fact is evidence by the comparison of the representative low-magnification TEM images of the initial GO, rGO, C-ny graphene, and C-xy graphene displayed in Figure 2b. TEM imaging of both GO and rGO, demonstrates the absence of any rips or holes, whereas for both C-ny graphene and C-xy graphene the formation of matrices of nanoscale holes is revealed due to the progressive C–C bonds cleavage upon GO conversion into these graphene derivatives discussed in detail in Refs. [28] and [29]. In C-ny graphene nanoholes with the average size of ≈ 2 –7 nm are densely distributed within the graphene layer, whereas in C-xy graphene holes are 10–50 nm in size separated by areas of pristine graphene of tens of nanometers. This governs the discussed difference in the π -conjugation degree in C-ny graphene and C-xy graphene. Tight localization of a large number of holes in C-ny graphene also results in corrugation of the graphene layer evidenced by the blurring of diffraction spots as is shown in the Figure 2c. No such effect is indicated for the C-xy graphene for which as for GO and rGO layers ED pattern is presented by a single set of narrow diffraction spots, asserting the monolayer and planar structure of the graphene layer.^[43]

Notably, the nanoscale perforation of C-ny graphene and C-xy graphene overall does not result in the disruption of graphene platelets as is seen from the exemplary SEM images of arrays of GO, rGO, C-ny graphene, and C-xy graphene platelets in Figure 2d. The analysis of the size distributions of the studied graphene derivatives performed by means of laser diffraction (LD) method and processing of arrays of SEM images (Section S1,

Supporting Information) has revealed that the lateral size of the platelets retains almost unchanged, lying within the range of 3–100 μm . The equality of the lateral size of the studied graphene derivatives is of high importance since the size effect can substantially affect the electronic structures of the graphenes and distort the analysis of the effect of the chemical functionalization on the VB structure.^[3,4,44] **Figure 3** highlights the key features of the chemistry and morphology of the graphene derivatives under study.

Acquiring the areas of the spectral components obtained upon C 1s and O 1s spectra fitting, the relative concentrations of respective functional groups and carbon in various states have been estimated. The quantitative data are presented in **Table 1** and Section S2, Supporting Information. GO is predominantly functionalized by the basal-plane hydroxyls and epoxides, which in relative concentration is estimated to be 43.3 at%, and contains a certain amount of ketones (4.3 at%) and carboxyls (4.3 at%). Conversion of GO into rGO has resulted in almost complete elimination of oxygen moieties with their relative concentration becoming less than 0.1 at%. In turn, ketones and carboxyls are the main oxygen groups represented in the C-ny graphene (6.9 at%) and C-xy graphene (7.2 at%), respectively, with the almost complete absence of the basal-plane hydroxyls and epoxides. However, the chemistry of both C-ny graphene and C-xy graphene is not completely homogeneous. Both materials contain some amount of retained and formed edge-located hydroxyls/ethers formed during the synthesis process and the retained carboxyls/ketones. In the C-ny graphene, ketones present almost 60% of all the oxygen moieties, whereas in the C-xy graphene this value is $\approx 63\%$. Nevertheless, despite the presence of some residual oxygen groups, the dominance of ketones and carboxyl groups results in the appearance of a set of spectral features in the VB photoelectron spectra, which can be clearly discerned and analyzed.

Figure 4a displays valence band (VB) spectra of the GO, rGO, C-ny graphene, and C-xy graphene. The measured VB spectra were double differentiated, which allows one to unveil broadened, over-lapping spectral features, and precisely determine

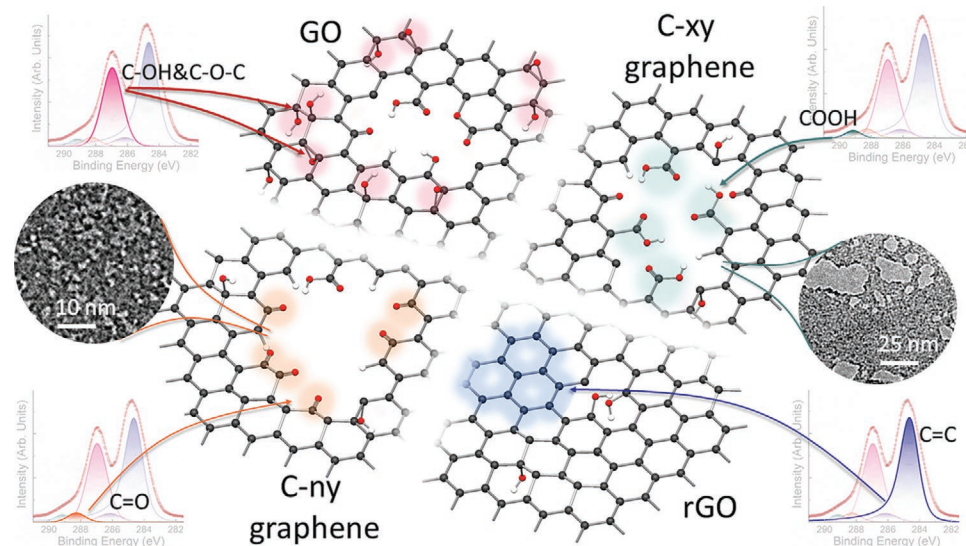


Figure 3. Schematic representation of C-ny graphene, C-xy graphene, GO, and rGO.

Table 1. Relative content of different chemical groups in the studied graphene derivatives.

Component	C=C	C–OH(ph)	C–OH&C–O–C	C=O	COOH	C=O/C _{oxi}	COOH/C _{oxi}
	Binding energy [eV]	284.6	286.3	286.8	288.1	288.8	
Graphene derivatives	GO	48.1	<0.1	43.3	4.3	4.3	8.3%
	rGO	>99	<0.1	<0.1	<0.1	<0.1	<0.1
	C-ny	85.1	4.2	<0.1	6.9	2.7	60%
	C-xy	86.4	3.7	<0.1	1.6	7.2	13.9%

their positions.^[45] The second derivative spectra of GO, rGO, C-ny graphene, and C-xy graphene taken with the opposite sign ($-d^2I/dE^2$ curve) are presented in Figure 4b. All VB spectra are presented by a set of spectral features denoted as A–G', revealing the fine structure of density of electronic states related to σ and π orbitals of graphene lattice and oxygen groups. The relative intensity of these spectral features is determined by two factors: i) the abundance of the corresponding orbitals in the studied CMG owing to its chemistry and structure; and ii) cross-section for photoexcitation of electrons occupying the corresponding states, including its dependence on the angle α between the electric field vector E and the axis of the orbital. In the performed studies the magic angle was preset $\alpha = 54.7^\circ$, ensuring almost equal excitation of the in-plane σ -related states and out-of-plane π -related states.

As seen, the functionalization of graphene by ketones or carboxyl groups results in the substantial modification of the VB DOS across all the BEs. The appearance of the narrow H peak with BE ≈ 31 eV in the VB spectra of C-ny graphene and C-xy graphene is attributed to the $2p$ line manifestation of the sodium atoms (Na $2p$) retained in trace amounts after the synthesis of these CMGs.^[29,46] Notably, although being less intensive, the spectral feature H reveals also in the initial GO and rGO as well, which is particularly seen from the second derivative spectra (Figure 4b). The Z peak in the rGO VB spectrum located at the BE of 24.6 eV originates from the appearance of the C $1s$ line excited by the photons with the energy of 390 eV corresponding to the incompletely damped third order of diffraction generated by a plane grating monochromator of the

beamline. Besides these spectral features, a broad G peak centered at BE ≈ 26 eV is distinguished in all the oxygen-functionalized CMGs. The analysis of the 2nd derivative spectra also reveals that this peak is accompanied by a less-intensive G' peak with BE of ≈ 28.4 eV. Both of these spectral features correspond to O $2s$ related electronic states contributed from all oxygen-containing functionalities, resulting in their relatively large widths with FWHM ≈ 3.5 eV. This interpretation is confirmed by the absence of G and G' peaks in the spectrum of rGO, in which almost all the oxygen moieties are eliminated according to the XPS data (Table 1). Moving to an intermediate region of ranging from 12.5 to 22.5 eV, the D , E , and F peaks with BEs of ≈ 13.6 , ≈ 17.0 , and ≈ 19.5 eV are to be distinguished, most prominently revealing themselves in the VB spectrum of rGO. Accordingly, they are assumed to be related to purely graphenic spectral bands, arising due to the next four high-symmetry points of graphene Brillouin zone according to the performed calculations of the graphene DOS and published data:

$K_1^+(\sigma_3)$ for feature D , converged $K_3^+(\sigma_3)$ and $M_{1u}^+(\sigma_2)$ states for feature E , and $M_{1g}^+(\sigma_1)$ for feature F .^[25,47,48] It is worth noting that other interpretation of these features can be also found in the published data ($Q_{1u}^+(\sigma)/P_3^+(\sigma)$, $Q_{1g}^+(\pi)$, and $\Gamma_{1g}^+(\sigma)$ for features D – F , respectively),^[17] although the graphene nature of these states is indisputable. In turn, the prominent A' feature centered at BE of ≈ 3.2 eV in the rGO VB spectrum is attributed to the contribution of the π states (Q_{2u}) of the graphene network.^[16,17]

Besides the rise of the Na $2p$ related spectral feature H , the most prominent changes in the VB DOS of graphene upon its

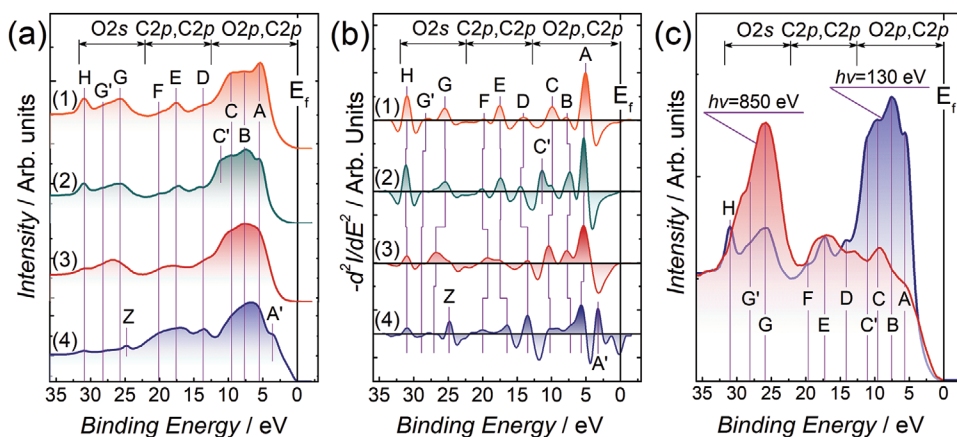


Figure 4. VB spectra of graphene derivatives. a) The initial and b) negative doubly differentiated VB spectra of C-ny graphene (1), C-xy graphene (2), GO (3), and rGO (4). c) VB spectra of C-xy graphene acquired with the excitation energies of $h\nu = 850$ eV and $h\nu = 130$ eV.

chemical derivatization are expressed by the appearance of the well-defined A' , A , B , C , and C' spectral features. These bands are both absent in the VB spectrum of rGO and hardly resolved in the DOS of GO, owing to the mixed composition of ketones and carboxyl groups along with the presence of basal-plane hydroxyls and epoxides. The comparison of the VB spectra measured at the photon energies of $h\nu = 130$ and $h\nu = 850$ eV displayed in Figure 4c reveals the $2p$ origin of these spectral features. In the case of the excitation energy of $h\nu = 130$ eV the cross-sections of $2p$ and $2s$ states are almost equal, whereas in the case of $h\nu = 850$ eV the cross-section of $2p$ states is substantially lower compared to the $2s$ one. Thus, the observed diminishing of the DOS in at BEs below ≈ 13 eV upon moving to $h\nu = 850$ eV verifies the $2p$ nature of the A , B , and C (C') spectral features.

Comparative analysis of VB spectra of C-xy graphene and C-ny graphene prior to and after higher temperature annealing at $T = 345$ °C for 2 h further verified that the defined A , B , and C (C') features are related to the presence of ketones and carboxyl groups. Figures 5a and 5b display the acquired VB spectra (curves 1 and 2) with the result of their subtraction (curve 3). Upon annealing the elimination of ketones and carboxyl groups proceeds (Figure 5c) with the simultaneous substantial reduction of the DOS in the region of 5–12.5 eV. A single broad band at BE ≈ 8 eV attributed to the $C2p$ states of a pristine graphene lattice retains after the treatment.^[17,25,26] At the same time, the well resolved A – C (C') features disappear, signifying they originate from the ketones and carboxyl groups for both C-ny graphene and C-xy graphene. Moreover, even though the relative concentration of these oxygen groups is not exceeding 8 at%, the impact of the states related to these functionalities on the VB spectra is quite solid: changes in the integral intensity after annealing are of ca. 30% and 40% for C-ny graphene and C-xy graphene, respectively. This originates from the fact that the total cross-section for the photoionization of oxygen atomic $2p$ orbitals at $h\nu = 130$ eV is ≈ 8 times larger than that for the photoionization of carbon $2p$ orbitals.^[49] Note that analogously to the A – C (C') bands, G and G' features disappear upon the thermal annealing, justifying their assign to O $2s$ related electronic states. The absence of the A – C (C'), G , and G' bands also asserts that these spectral features are not related to the

introduction of a matrices of holes introduced to graphene layer upon the nanoscale perforation which retain after the applied thermal annealing.

To figure out the origin of the A – C (C') spectral features in terms of the atom and molecular-related states in ketones and carboxyl groups both empirical and theoretical studies were performed. A facile approach has been proposed based on the analysis of the electronic structure of a certain functional group by means of the data on the electron configuration, sequence of energy levels, and nomenclature (notation) of molecular orbitals for a model organic molecule, which possesses a stereochemical structure similar to an examined moiety. Within the frame of such a methodology, formaldehyde (H_2CO) and formic acid ($HCOOH$) molecules, of which the electronic structure was thoroughly studied both experimentally and theoretically,^[50–54] were used as model systems for ketones and carboxyl groups in C-ny graphene and C-xy graphene, respectively. Structure of the chosen model molecules and the respective functional groups differs only in the replacement of $\sigma(C-H)$ bonds in former ones by respective $\sigma(C-C)$ bonds in latter ones. This alteration does not affect the bonding configuration within the atoms of both molecules and functional groups and does not affect the symmetry of moieties. Thus, the symmetry of formaldehyde molecule described by C_{2v} point group practically retains in the case of the ketone in C-ny graphene, while the simpler symmetry of formic acid molecule represented by C_s point group completely repeats in the case of carboxyl group. It is worth noting that in the case of C-ny graphene, the $\pi(C=O)$ bond can conjugate with the π -system of the graphene network, which will result in the broadening of the corresponding electronic states and their possible diminishing in the VB spectra. This feature reveals itself in the subsequently performed theoretical calculations. It is worth noting that hydroxyl group can conjugate with the π -system of graphene as well, although being a π -electron donor unlike the π -electron acceptor behavior of carbonyls. However, due to low concentration of isolated hydroxyls in C-ny and C-xy graphene along with the aforementioned broadening of states related to π -conjugated system, we neglect this factor.

Given this, the comparative analysis of the VB spectra of C-xy/C-ny graphene and respective model molecules was

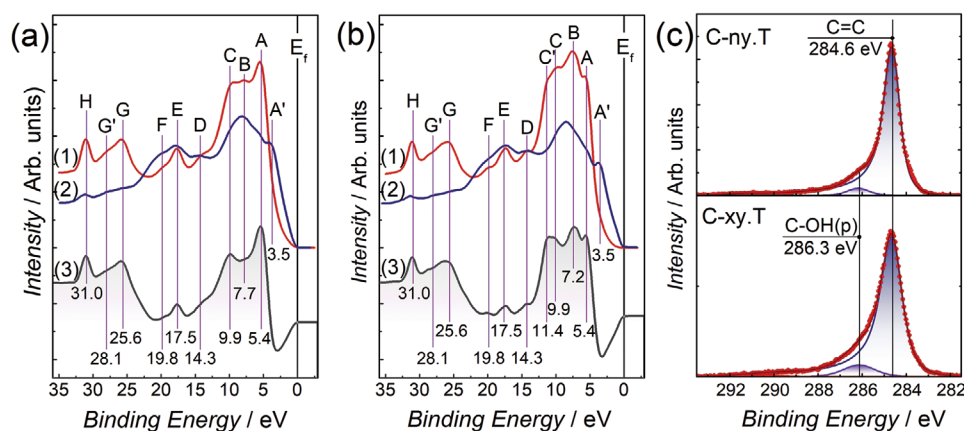


Figure 5. VB modification upon annealing. VB spectra of a) C-ny graphene and b) C-xy graphene prior to (1) and after (2) the thermal annealing with the result of their subtraction (3). c) C 1s photoelectron spectra of the annealed C-ny graphene and C-xy graphene.

Table 2. The assignment of the VB features in C-ny graphene.

Formaldehyde (H ₂ CO) (gas phase data) ^[42]			C-ny graphene (this work data)		
MO label (symmetry type)	BE [eV] with respect to E_V (E_F)	MO nature	VB feature	BE [eV] with respect to E_F	Assigned electron states of C-ny graphene
$2b_2$	10.9 (5.0)	$n'(O2p_x)$	A	5.0	$n'(O2p_x)$
$1b_1$	14.5 (8.6)	$\pi(CO)$	B	7.6	$\pi(CO)$
$5a_1$	16.1 (10.2)	$\sigma(CO)$	C	9.8	$\sigma(CO)$
$1b_2$	17.0 (11.1)	$\pi'(CH_2)$			
$4a_1$	21.4 (15.5)	$\sigma(CH_2)$			
			D	14.0	$\sigma(C=C)$ (graphene)
			E	17.4	$\sigma(C=C)$ (graphene)
			F	19.8	$\sigma(C=C)$ (graphene)
$3a_1$	34.2 (28.3)	$\sigma(CO)$	G	25.4	$\sigma(CO)$
			G'	28.2	

performed, allowing us to assign the A–C(C') features to the corresponding states in the ketones or carboxyl group. **Tables 2** and **3** display the results of such an interpretation of the oxygen-related states in the VB spectra of the C-ny and C-xy graphene. The special symbols denoting the VB states and energy levels of formaldehyde and formic acid molecules are related to the irreducible representations of respective point groups and contain information both on the symmetry type of particular MO (second position) and on its ordinal number in the row of the orbitals of the same symmetry (first position). Particularly, a_1 , a_2 , b_1 , or b_2 symbols denoting orbitals of formaldehyde are traditionally used to designate four different irreducible representations of C_{2v} point groups. Accordingly, symbols a' and a'' included in notations of formic acid MOs are used to denote two irreducible representations of C_s point groups. The type (symbol) of irreducible representation of particular point group completely defines how the respective orbital is transformed under each included in this group symmetry operations and, thus, completely determines all symmetry properties of the

orbital. Quite similar approach has been also used for notation of the main peaks appearing in the VB spectra of C-ny graphene and C-xy graphene.

As seen from Table 2, in the case of C-ny graphene, the feature A with BE ≈ 5.1 eV is determined to arise from the MOs occupied by oxygen 2p nonbonding lone pair electrons n'_{O2p} (HOMO). Features B and C are attributed to π''_{CO} (HOMO-1) and σ'_{CO} (HOMO-2) MOs arising from π and σ bonds within C=O group, respectively.^[50,51,53] In C-xy graphene the nature of A, B, C, and C' features are more complex since six electronic states in the DOS spectrum of the formic acid measured in the gas phase are to be associated with four spectral features in the VB spectra.^[54] However, as was demonstrated by the measurements of the VB spectra of the layers of deposited formic acid condensation of the molecules results in the merging of the adjacent spectral bands due to the association of the MO electron pairs with the close BEs.^[47] Taking this into account, the A band in the C-xy graphene VB was assigned to the MOs occupied by oxygen 2p lone pair electrons in carbonyl and hydroxyl

Table 3. The assignment of the VB features in C-xy graphene.

Formic acid (H(CO)OH) (gas phase data) ^[45,47]			C-xy graphene (this work data)		
MO label (symmetry type)	BE [eV] with respect to E_V (E_F)	MO nature	VB feature	BE [eV] with respect to E_F	Assigned electron states of C-xy graphene
$10a'$	11.5 (6.7)	$n'(O2p)$	B	7.2	$n'(O2p)$
$2a''$	12.6 (7.8)	$\pi_2(CO), n''(OH)$	B	7.6	$\pi_2(CO), n''(OH)$
$9a'$	14.8 (10.0)	$\sigma(CO), n'(OH)$	C	9.7	σ'_{CO}
$1a''$	15.8 (11.0)	$\pi_1(OCO)$	C'	11.1	$\pi_1(OCO)$
$8a'$	17.1 (12.3)	$\sigma(OCO), \sigma(OH)$			$\sigma(OCO), \sigma(OH)$
$7a'$	17.8 (11.2)	$\sigma(CO), \sigma(OH), \sigma(CH)$			
$6a'$	22.0 (17.2)	$\sigma(CO), \sigma(OH)$			
			D	14.1	$\sigma(C=C)$ (graphene)
			E	17.2	$\sigma(C=C)$ (graphene)
			F	19.8	$\sigma(C=C)$ (graphene)
$5a'$	30.7 (25.9)	$\sigma(CO)$	G	25.3	$\sigma(CO)$
$4a'$	33.0 (28.2)	$\sigma(CO)$	G'	28.7	$\sigma(CO)$

fragment of a carboxyl group, n'_{O2p} and n_{OH} , with a probable contribution from a π'_{CO} MO. Feature B was attributed to the mix of π'_{CO} MO and σ'_{CO} MO in C=O part of a carboxyl group, whereas feature C is concerned to arise from the sum of σ'_{OCO} and σ'_{OH} MOs related to σ -bonding within the group. Finally, C' band is attributed to the additional states, originating from σ_{CO} , σ_{OH} , and σ_{C-C} MOs of the carboxyl group. Note that the position of G and G' features also match with O2s states positioned at BE ≈ 26 –28 eV in the DOS spectra of both formaldehyde and formic acid, verifying the assumed assignment.

The results of the applied empirical approach are supported by the theoretical modeling performed using Vienna Ab-initio Simulation Package (VASP).^[55] The fundamental background of the applied modeling procedure is thoroughly described in Section S3, Supporting Information. Technical details of DFT modeling are presented in Experimental section. We calculated the electronic structure of two model systems, as shown in Section S4, Supporting Information, and obtained projected densities of states (pDOS) and electron densities. To reveal the effect of ketones and carboxyl groups on the electronic structure, we have calculated the sums of all pDOS on atoms of the corresponding functional groups, which are further denoted as the total projected densities of states (TpDOS). **Figure 6** displays TpDOS and images of the electron density distributions (EDD) calculated for the: a) ketone in C-ny graphene (C-ny TpDOS) and model formaldehyde molecule; b) carboxyl group in C-xy graphene (C-xy TpDOS) and model formic acid molecule. TpDOS both calculated for model molecules and C-ny and C-xy graphene were moved to higher energies by 4.6 eV. Figure 6a displays that the calculated C-ny TpDOS is presented by a set of bands positioned at BEs of ≈ 5.3 , ≈ 9.6 , and ≈ 25.4 eV, which one-to-one correspond to the A, C, and G peaks in the experimental VB spectra of C-ny graphene and to $2b_2$, $5a_1$, and $3a_1$ states in the DOS of formaldehyde. At the same time, no band is observed in the calculated C-ny TpDOS within the range of 6–8.3 eV, where B feature in the experimental VB spectra and $1b_1$ state of the calculated DOS of formaldehyde lie. This originates from the fact that $\pi(C=O)$ bond in the modeled C-ny

graphene, to which the MO in this state is attributed, is conjugated with the system of π -states of the graphene network. This leads to a substantial broadening of the π'_{CO} state and, hence, its diminishing in the calculated TpDOS. In formaldehyde, apparently, the π -conjugated system is absent and the π'_{CO} state is localized and well defined. At the same time, in the experimentally studied C-ny graphene the conjugation of the $\pi(C=O)$ bond is still partially suppressed by the disruption of π -bonding due to covalent functionalization of the adjacent carbon atoms by the retained hydroxyl groups. This results in the presence of a notable B feature related to π'_{CO} states, although its intensity is sufficiently low is thanks to the small number of the unconjugated ketones.

The calculated C-xy TpDOS is comprised by the set of bands lying at BEs of ≈ 7.1 , ≈ 7.8 , ≈ 9.5 , ≈ 11.1 , ≈ 11.7 , ≈ 25.5 , and ≈ 27.8 eV (Figure 6b). The pairs of bands with BEs of ≈ 7.1 and ≈ 7.8 eV comply with the $10a'$ and $2a''$ states in the DOS of the formic acid and in a mixed form refer to the B feature in the VB spectrum of C-xy graphene. Analogously, bands positioned at BEs of ≈ 11.1 and ≈ 11.7 eV correspond to $1a''$ and $8a'$ states of the formic acid and merged are represented by a C' feature in the VB spectrum of C-xy graphene. Finally, the band at ≈ 9.5 eV one-to-one corresponds to the $9a'$ state in the DOS of a model formic acid molecule and C band in the experimental VB spectrum.

Apart from approving the previously made assignment of the VB A, C, and G spectral features, the carried out comparative analysis also allows to estimate the types of symmetry of the MOs of ketones and carboxyl groups. The MOs in the ketone have b_2 , a_1 , and a_1 types of symmetry, being analogous to the ones in formaldehyde. Thus, the notation of these states by the symbols $3a_1$, $4a_1$ and $1b_2$ can be applied. In the same way, five bands of C-xy TpDOS are attributed to the a' symmetry type ($9a'$, $8a'$, $7a'$, $6a'$, $5a'$, $4a'$), and two bands are qualified as the ones of a'' type ($2a''$, $1a''$). The provided assignment of the symmetry types for MOs is supported by the analysis of the corresponding EDD images. The a_1 type of MO symmetry implies that the spatial distribution probability density remains the same after the following symmetry operations of C_{2v} point

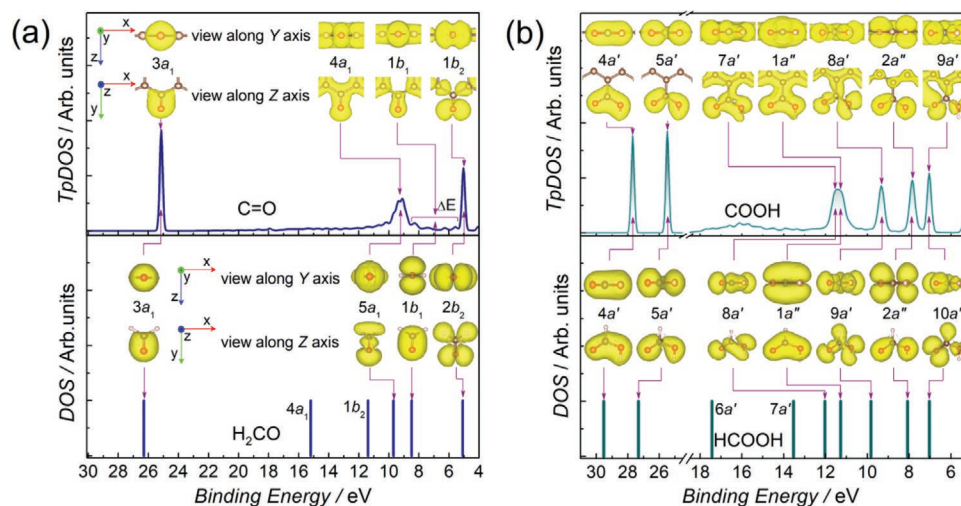


Figure 6. Comparison of the DOS for model molecules and TpDOS for the corresponding functional groups in graphene derivatives. a) DOS of formaldehyde and TpDOS of the ketone. b) DOS of formic acid and TpDOS of the carboxyl group.

group: C_2 - rotation around symmetry axes Y on angle 180° ; σ_{xy} - reflection in mirror plane xy ; σ_{yz} - reflection in mirror plane yz .^[56] In turn, b_1 and b_2 types of symmetry signify that electron probability amplitude remains the same after C_2 operation, but change its sign after σ_{xy} and σ_{yz} operations, respectively. As seen, images of EDDs corresponding to $1b_1$ band and $1b_2$ peak of C-ny TpdDOS are divided by xy and yz nodal planes into two mirror-symmetrical parts. For C-xy TpdDOS, electron states with a' symmetry also demonstrate the in-plane character of their EDD, while the ones with a'' symmetry consisting of two mirror-symmetrical parts divided by a nodal plane, the xy -plane in our case. Details on the notation of ketones and carboxyl groups are presented in Section S5, Supporting Information.

Figure 7 displays the contributions in C-ny and C-xy TpdDOS of the projected DOS on $2s$, $2p_x$, $2p_y$, and $2p_z$ atomic orbitals (AO), allowing finally determine their origin in terms of atomic and molecular states. As seen, the $1b_2$ state of C-ny TpdDOS takes the form of a single $O2p_x$ AO, whereas in the C-xy TpdDOS $9a'$ state corresponds to the sum of $O2p_x$ and $O2p_y$ AOs. In both cases, these AOs refer to the nonbonding lone pair orbitals in oxygen atoms of ketones and carboxyl groups that are clearly seen in the corresponding EDD images.^[57] The band $4a_1$ in C-ny TpdDOS reveals itself in the $2s$ and $2p_y$ AOs of carbon and oxygen atoms known to give rise to bonding $\sigma(C-O)$ orbital. This coincides with the predominant distribution of the electron density along the C-O axis of the ketone pointed out by the corresponding EDD image. The substantially broadened $1b_1$ band of the C-ny TpdDOS is presented by $2p_z$ AOs of carbon and oxygen atoms, constituting $\pi(C=O)$ bond. This verifies to the aforementioned spreading of this band due to the extension of the corresponding energy levels upon conjugation of $\pi(C=O)$ bond with the network of $\pi(C=C)$ bonds of graphene network.

Moving to C-xy TpdDOS, the $7a'$ and $8a'$ states are seen to arise from the mix of $2s$, $2p_x$, and $2p_y$ AOs central carbon and two

terminal oxygen atoms. This combination of AOs corresponds to 4-center σ -type bonding, analogously to the formic acid molecule, where the formation of this σ bonds is manifested by $8a'$ and $9a'$ states. In turn, the $1a''$ and $2a''$ bands come from out-of-plane $2p_z$ AOs. The $2a''$ band has the form of a superposition of nonbonding O $2p_z$ orbital of hydroxyl oxygen and bonding $\pi(C-O)$ orbital formed via overlap of ketone's C $2p_z$ and O $2p_z$ orbitals. At the same time, $1a''$ MO is a multicenter (3-center) π -bonding orbital with out-of-plane geometry. Finally, $3a_1$ state in C-ny TpdDOS along with $4a'$ and $5a'$ states in C-xy TpdDOS are demonstrated to originate predominantly from $O2s$ AO with some impact from $2p_y$ AO of carbon and oxygen atoms in the case of C-ny TpdDOS, and $2p_x$ plus $2p_y$ AOs of carbon and oxygen atoms in the case of C-xy TpdDOS. The contribution of $2p$ AOs from carbon atoms is asserted to arise due to the peculiarities of the applied projection and can be neglected.

As a net result, the performed theoretical calculations fully verify the relevance of identifying the states related to ketones and carboxyl groups by means of the comparison of the examined VB spectra with the DOS spectra of the model formaldehyde and formic acid molecules, respectively. Figure 8 summarizes the interpretation of all the features in the VB spectra of C-ny graphene and C-xy graphene, arising from both the electronic states of the modifying groups and graphene network represented by the theoretically calculated C-ny and C-xy TpdDOS spectra as well as the DOS of graphene lattice. It should be noted that for better coincidence, rGO TpdDOS was stretched along BE axis by 1.4 times and C-ny and C-xy TpdDOS were moved to higher energies by 4.3 and 4.6 eV, respectively. As seen, the A-G' spectral features match up nicely to the assigned states in the theoretical DOS spectra. Moreover, the comparison of the presented spectra gives a consistent explanation of the presence of A spectral feature in the VB spectra of C-xy graphene and G' feature in the VB spectra of C-ny graphene. The appearance of these bands related solely to ketone

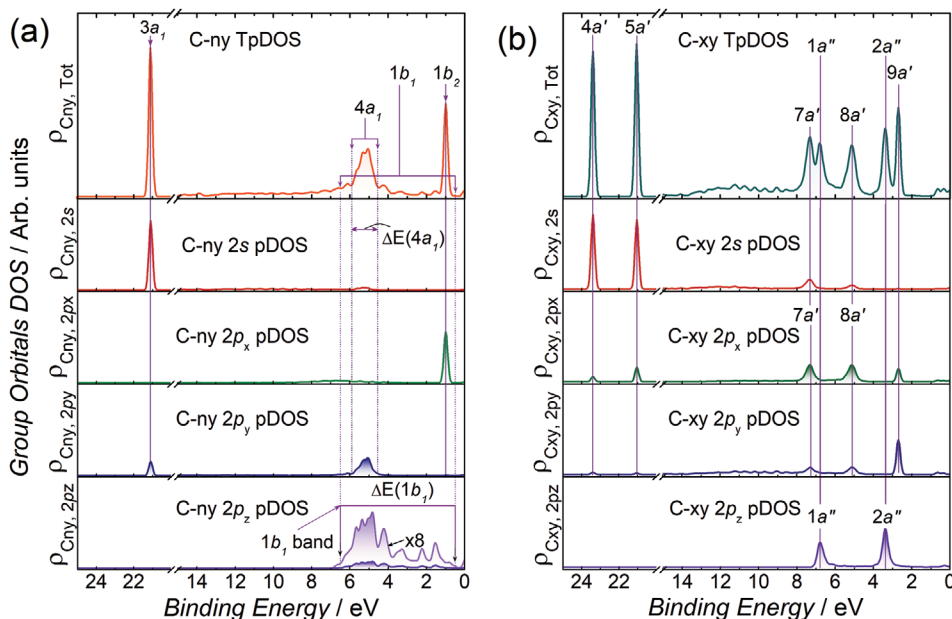


Figure 7. Calculated TpdDOS and its projection on the $2s$, $2p_x$, $2p_y$, and $2p_z$ AOs for a) ketone and b) carboxyl group.

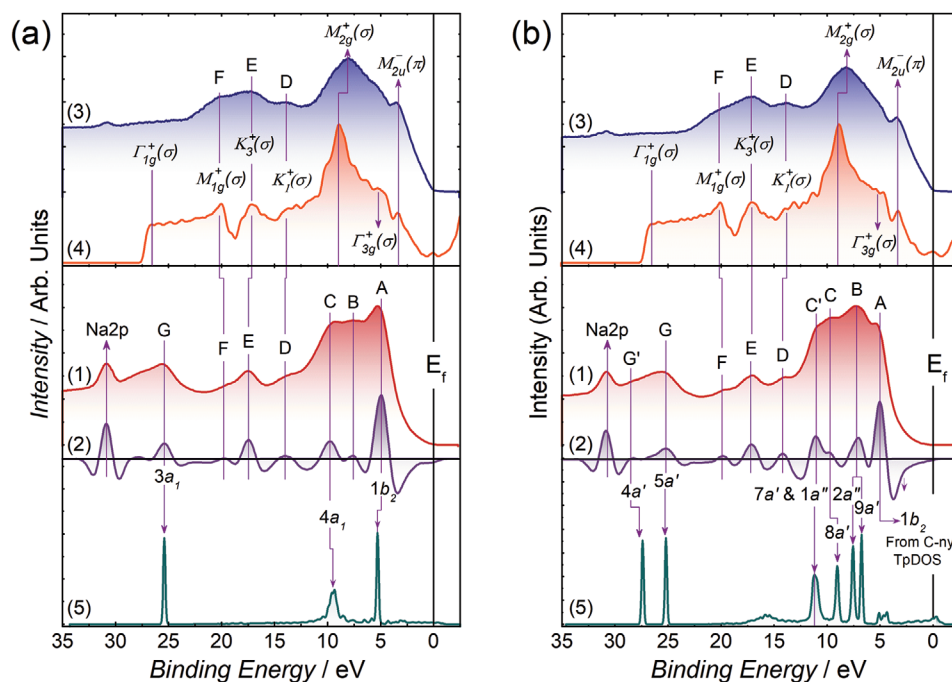


Figure 8. The experimental VB spectra (1), its second derivative (2), VB spectra after annealing (3), theoretical DOS spectra of graphene (4), and TpDOS of the modifying group (5) for a) C-ny graphene and b) C-xy graphene.

and carboxyl group is due to their presence to some extent in the C-xy graphene and C-ny graphene, respectively (Table 1). This fact implies that the analysis of VB spectra of graphene derivatives also allows one to specify the analysis of the chemistry of material via XPS studies.

3. Conclusion

Thus, we show that covalent functionalization of graphene layer results in a substantial modification of its VB with the appearance of localized states related to MOs of the modifying functionalities. The proposed empirical approach of applying model molecules as references provides the basis to predict and analyze the impact of certain modifying functionality on the band structure of graphene. Both empirical analysis and DFT calculations by means of using projection of the total DOSs on the atoms of the modifying group allow to decompose the impact of the localized states corresponding to non-bonding lone pair electrons n_{O2p} , σ , and π bonds. This is of high interest within the frame of designing the graphene-based catalysts, organic photovoltaic devices, and sensing systems. We demonstrated that the VB of graphene chemical derivatives can be viewed as a superposition of the graphene DOS and molecular-like states of the modifying group unless they are not related to π -bonding. In this case, the corresponding states are embedded into the delocalized system of the π -conjugated graphene network. The revealed similarity of molecular-related states in the CMGs and model molecules also allowed us to propose the usage of the nomenclature for the notation of these states, pointing out their symmetry type, analogous to one used for organic molecules. The presented results highlight graphene functionalization by

a certain organic group to be an advanced tool for engineering its electronic structure, complementing the common studies on the use of graphene derivatization for the alteration of its bandgap. Moreover, the analysis of VB of graphenic materials can be regarded as a powerful tool to elucidate not only the electronic structure but their chemistry as well, owing to its sensitivity to the introduction of certain organic molecules. Taken together, our findings guide the band structure engineering of graphene derivatives, both solely and as a part of Moiré structures, taking advantage of combining graphene derivatives with variously altered VB DOS.

4. Experimental Section

Materials: An aqueous dispersion of graphene oxide was purchased from Graphene Technologies (Russia, www.graptechrus.com). Sodium silicate (99%, p.a.) was obtained from Merck KGaA, Germany. Argon of 99.999% purity was obtained from NevaPromGas, Ltd., Russia.

Synthesis Procedure for C-ny Graphene: C-ny graphene was synthesized according to the method described in Ref. [29]. GO aqueous dispersion (30 mL of 0.3 wt%) was poured into a fluoroplastic cup. Then sodium silicate powder was added while stirring to reach pH = 9 in the resulting mixture. The pH values of the suspensions were evaluated with a Fisher Scientific Accumet Basic AB15 pH meter (Thermo Fisher Scientific, USA). The obtained suspension was further heated at $T = 80^\circ\text{C}$ for 48 h in the air. Afterwards, the resulting mixture was cooled to room temperature and copiously washed via centrifugation (Sigma S-16 centrifuge, Germany) at 18 200 g for 15 min. with sequential rinsing of the obtained sediment at distilled water (30 mL). The described purification procedure was repeated few times to obtain an aqueous suspension of C-ny graphene platelets.

Synthesis Procedure for C-xy Graphene: C-xy graphene was synthesized according to the method described in Ref. [28,58]. GO film deposited on the desired substrate (silicon/quartz wafer, TEM grid, multisensory

chip, etc.) via drop-casting was placed onto the quartz window in the bottom of the sealed cylindrical reactor of ca. 35 cm³ of volume with entries for gas flow input and output at the top. The reactor was housed on the top of deuterium lamp L6565 (Hamamatsu, Japan) with the maximum intensity at $\lambda = 210$ nm ($E = 5.90$ eV). The distance between the sample surface and the lamp was 11 mm. Prior to the photochemical modification, the reactor was purged by a 150 sccm flow of pure argon gas during 10 min. Afterwards, the deuterium lamp was turned on and the GO film was exposed to UV radiation during 20 min. with the constant flow of argon, resulting in the conversion of GO into C-xy graphene according to the mechanism described in Ref. [58]. The temperature of the sample during the irradiation has not exceeded $T = 35$ °C.

Synthesis Procedure for rGO, Annealed C-xy Graphene, and C-ny Graphene: The rGO samples were prepared by thermal annealing of a GO film on a silicon wafer at $T = 800$ °C in the ultra-high vacuum chamber ($P = 10^{-9}$ Torr) for 4 h. The annealing of the C-xy graphene and C-ny graphene was performed at $T = 650$ °C in the ultra-high vacuum chamber ($P = 10^{-9}$ Torr) for 2 h.

Materials Characterization: The XPS and VB spectra were acquired at the Russian-German beamline (RGLB) of electron storage ring BESSY-II at Helmholtz-Zentrum Berlin (HZB), using the ultrahigh vacuum experimental station.^[59] For each studied material, the X-ray photoelectron spectra were collected in four different areas of the sample for the following processing. Prior to the measurements, all samples were placed at a chamber evacuated down to a pressure $P = 10^{-9}$ Torr for 6 h to remove all adsorbates.

The recorded X-ray photoelectron spectra were calibrated in accordance with the position of the reference Au 4f_{7/2} line (84.0 eV). In the case of low-conducting GO films, the positions of the C 1s and O 1s lines shifted due to the surface charging effect were corrected by the additional shift with respect to the same lines of the rGO.

CasaXPS@ software (Version 2.3.16Dev52, Casa Software Ltd.) was used to deconvolute and to subsequently quantify the recorded C 1s and O 1s high-resolution spectra. All the spectra were fitted with Shirley background. For C-ny, C-xy and r-GO C 1s spectra the best fitting result was achieved using six or less symmetric Gaussian–Lorentzian lineshapes GL(60) (Gaussian by 40% and Lorentzian by 60%) and one asymmetric Lorentzian Finite lineshape LF(α, β, w, m) with values of its α, β, w , and m parameters equal to 0.42, 0.82, 230, and 700, respectively. For GO C 1s spectrum as well as for all O 1s spectra the best fitting results were obtained while using only symmetric lineshapes GL(n) with parameter n ranging from 40 to 60. The deconvolution procedure was performed until the best agreement between the experimental spectra and their fitting was achieved applying nonlinear least-squares routine. Afterwards, the C/O ratios, relative concentration of the carbon atoms in different states were calculated for all the spectra acquired for each material and averaged to yield the reported values.

To check the reliability and inter-consistency of the fitting results obtained separately from C 1s and O 1s spectra (C=O)/(C–O) ratios for both types of spectra were calculated. The values of these ratios were obtained using Equation (1) for C1s spectra and Equation (2) for O 1s spectra:

$$\frac{(C=O)}{(C-O)}_{C1s} = \frac{A_{C1s}(COOH) + A_{C1s}(C=O)}{A_{C1s}(COOH) + A_{C1s}(C-OH \& C-O-C)} \quad (1)$$

$$\frac{(C=O)}{(C-O)}_{O1s} = \frac{A_{O1s}(C=O)}{A_{O1s}(C-O)} \quad (2)$$

In both formulas symbols $A_{C1s}(X)$ and $A_{O1s}(Y)$ designate the areas of X and Y components of C1s and O1s spectra, respectively. The values of (C=O)/(C–O) ratios calculated using these equations demonstrate a fairly good inter-consistency of the results obtained for the same samples. This fact, considering complete independence of data extracted from C 1s and O 1s spectra, provides serious evidence in favor of their high reliability.

The measurements of the X-ray photoelectron valence band spectra were performed along with the XPS studies at the incident photon energies of $\hbar\omega = 130$ and $\hbar\omega = 850$ eV. To provide a convenient comparison all the spectra were accurately smoothed (in order to eliminate stochastic noise), normalized to the equal intensity of the dip between O 2s peak and higher spectral features.

C K near-edge X-ray absorption fine-structure spectra were collected in the total electron yield mode by changing the incident photon energy and simultaneously recording the sample drain current. C K-edge XAS were collected within the range of $h\nu = 280$ –315 eV with a step of 0.1 eV. The measurements were performed at the beam incidence angle of 54.7°. The as-recorded spectra were further normalized and smoothed according to the conventional processing routine.^[60]

FTIR spectra were acquired using an InfraLUM-08 spectrometer (InfraLUM, Russia) equipped with the attenuation of total reflectance attachment.

For all the spectroscopic measurements CMG films on the silicon wafers were applied prepared by the drop-casting of 20 μ L of the aqueous and isopropyl suspension of the corresponding CMG, of 5×10^{-3} wt% of concentration, with the subsequent drying overnight at room temperature.

The morphology of the studied materials was investigated via LD measurements, TEM imaging, ED measurements, and SEM imaging. LD measurements of the GO aqueous suspensions were carried out with the use of Mastersizer 2000 (Malvern Panalytical, Great Britain). The complex refractive index for GO was set as $2.3 + 0.01i$ according to published data,^[61] and the Fraunhofer model was chosen for the scattering pattern processing as the most appropriate for the 2D GO platelets.^[62]

TEM images and ED patterns were acquired using the Jeol JEM-2100F microscope (Jeol, Japan) at the accelerating voltage of 200 kV. Samples for TEM studies were prepared by wetting the TEM Cu grid (400 MESH) in an aqueous suspension of the studied material of 0.01 wt% of concentration. SEM images were acquired using a JSM-7001F microscope (Jeol, Japan). Arrays of platelets of the graphene derivatives for the SEM imaging were obtained by Langmuir–Blodgett deposition the corresponding suspension (20 μ L, 0.01 wt%) over silicon wafers (5 \times 7 mm) followed by drying overnight at $T = 20$ °C in the air.

DFT Modeling: To reveal the electronic structure of functionalized graphene, the authors used periodical DFT calculations as implemented in Vienna Ab-initio Simulation Package.⁴⁷ The projector-augmented wave (PAW) method was used with the Perdew, Burke, Ernzerhof (PBE) exchange-correlation functional.^[63,64] During the ionic optimization Γ -point approximation was used, while for static self-consistent calculations Brillouin zone sampling was increased to $11 \times 11 \times 1$ Monkhorst-Pack k -mesh.^[65] RMM-DIIS algorithm was used for ionic optimization with ionic and electronic convergence criteria of 0.02 eV \AA^{-1} and 10^{-4} eV,^[66] respectively. In self-consistent calculations electronic convergence criteria was 10^{-6} eV. In all calculations, plane-wave cutoff energy was set as 500 eV.

The detailed description of the theory, lying behind the calculations of the projected DOS is presented in Section S3, Supporting Information.

Supporting Information

Supporting Information is available from the Wiley Online Library or from the author.

Acknowledgements

V.V.S. and M.K.R. contributed equally to this work. The work of M.K.R., D.Y.S., V.V.S., and M.V.B. acknowledge financial support from the Russian Foundation for Basic Research for the XPS studies of graphene derivatives (grant No. 20-04-60458). V.V.S., M.K.R., D.Y.S., M.V.B., and A.V.S. thank Helmholtz-Zentrum Berlin (HZB) for the allocation of synchrotron

radiation beamtime and Russian-German Laboratory at HZB (Germany) and for the financial support of the XPS and XAS measurements. D.Y.S.'s work was partially supported by NRC "Kurchatov Institute". S.V.P.'s, V.A.K.'s, and S.A.K.'s work on DFT modelling was supported by the state assignment of JIHTRAS (Theme No. AAAA-A19-119022190058-2). S.V.P. and V.A.K. acknowledge the use of Zhores for obtaining the results of DFT modelling.^[67] The authors would like to thank D. Smirnov (TU Dresden) for assistance during the experiment at RGLB. They would like to thank Dr. D. A. Kirilenko and Dr. S. I. Pavlov for their assist in SEM and TEM studies. V.V.S. and M.K.R. primarily designed the study and supervised the research. M.K.R. and A.V.S. performed the synthesis of graphene derivatives and prepared the samples for the studies. V.V.S., M.K.R., D.Y.S., A.V.S., M.V.B., and M.B. proceeded XPS, XAS, FTIR, LD, TEM, and SEM measurements. S.V.P., V. A. K., and S. A. K. carried out DFT calculations. M.K.R. and V.V.S. co-wrote the manuscript with input from M.B., D.Y.S., S.V.P., and P.N.B. All authors have given approval to the final version of the manuscript.

Open access funding enabled and organized by Projekt DEAL.

Conflict of Interest

The authors declare no conflict of interest.

Data Availability Statement

Research data are not shared.

Keywords

2D materials, band structure engineering, derivatization, DFT calculations, electronic structure, Moiré materials

Received: July 21, 2021

Revised: September 16, 2021

Published online: October 27, 2021

- [1] E. Y. Andrei, D. K. Efetov, P. Jarillo-Herrero, A. H. MacDonald, K. F. Mak, T. Senthil, E. Tutuc, A. Yazdani, A. F. Young, *Nat. Rev. Mater.* **2021**, 6, 201.
- [2] M. Brzhezinskaya, O. Kononenko, V. Matveev, A. Zotov, I. I. Khodos, V. Levashov, V. Volkov, S. I. Bozhko, S. V. Chekmazov, D. Roshchupkin, *ACS Nano* **2021**, 15, 12358.
- [3] Q. Zeng, H. Wang, W. Fu, Y. Gong, W. Zhou, P. M. Ajayan, J. Lou, Z. Liu, *Small* **2015**, 11, 1868.
- [4] Z. Meng, J. Zhuang, X. Xu, W. Hao, S. X. Dou, Y. Du, *Adv. Mater. Interfaces* **2018**, 5, 1800749.
- [5] A. Hirsch, F. Hauke, *Angew. Chem., Int. Ed.* **2018**, 57, 4338.
- [6] Z. Liu, J. Li, X. Liu, *ACS Appl. Mater. Interfaces* **2020**, 12, 6503.
- [7] C. Backes, A. M. Abdelkader, C. Alonso, A. Andrieux-Ledier, R. Arenal, J. Azpeitia, N. Balakrishnan, L. Banszerus, J. Barjon, R. Bartali, S. Bellani, C. Berger, R. Berger, M. M. B. Ortega, C. Bernard, P. H. Beton, A. Beyer, A. Bianco, P. Bøggild, F. Bonaccorso, G. B. Barin, C. Botas, R. A. Bueno, D. Carriazo, A. Castellanos-Gomez, M. Christian, A. Ciesielski, T. Ciuk, M. T. Cole, J. Coleman, C. Coletti, L. Crema, H. Cun, D. Dasler, D. De Fazio, N. Díez, S. Drieschner, G. S. Duesberg, R. Fasel, X. Feng, A. Fina, S. Forti, C. Galiotis, G. Garberoglio, J. M. Garcia, J. A. Garrido, M. Gibertini, A. Götzhäuser, J. Gómez, T. Greber, F. Hauke, A. Hemmi, I. Hernandez-Rodriguez, A. Hirsch, S. A. Hodge, Y. Huttel, P. U. Jepsen, I. Jimenez, U. Kaiser, T. Kaplas, H. Kim, A. Kis, K. Papagelis, K. Kostarelos, A. Krajewska, K. Lee, C. Li, H. Lipsanen, A. Liscio, M. R. Lohe, A. Loiseau, L. Lombardi, M. F. López, O. Martín, C. Martín, L. Martínez, J. A. Martín-Gago, J. I. Martínez, N. Marzari, A. Mayoral, J. McManus, M. Melucci, J. Méndez, C. Merino, P. Merino, A. P. Meyer, E. Miniussi, V. Miseikis, N. Mishra, V. Morandi, C. Munuera, R. Muñoz, H. Nolan, L. Ortolani, A. K. Ott, I. Palacio, V. Palermo, J. Parthenios, I. Pasternak, A. Patane, M. Prato, H. Prevost, V. Prudkovskiy, N. Pugno, T. Rojo, A. Rossi, P. Ruffieux, P. Samori, L. Schué, E. Setijadi, T. Seyller, G. Speranza, C. Stampfer, I. Stenger, W. Strupinski, Y. Svirko, S. Taioli, K. B. K. Teo, M. Testi, F. Tomarchio, M. Tortello, E. Treossi, A. Turchanin, E. Vazquez, E. Villaro, P. R. Whelan, Z. Xia, R. Yakimova, S. Yang, G. R. Yazdi, C. Yim, D. Yoon, X. Zhang, X. Zhuang, L. Colombo, A. C. Ferrari, M. Garcia-Hernandez, *2D Mater.* **2020**, 7, 022001.
- [8] W. Yu, L. Sisi, Y. Haiyan, L. Jie, *RSC Adv.* **2020**, 10, 15328.
- [9] M. Pumera, Z. Sofer, *Chem. Soc. Rev.* **2017**, 46, 4450.
- [10] J. Cheng, C. Wang, X. Zou, L. Liao, *Adv. Opt. Mater.* **2019**, 7, 1800441.
- [11] W. C. Tan, K.-W. Ang, *Adv. Electron. Mater.* **2021**, 7, 2001071.
- [12] X. Yu, H. Cheng, M. Zhang, Y. Zhao, L. Qu, G. Shi, *Nat. Rev. Mater.* **2017**, 2, 17046.
- [13] K. A. Mkhoyan, A. W. Contryman, J. Silcox, D. A. Stewart, G. Eda, C. Mattevi, S. Miller, M. Chhowalla, *Nano Lett.* **2009**, 9, 1058.
- [14] C. Gomez-Navarro, J. C. Meyer, R. S. Sundaram, A. Chuvilin, S. Kurusch, M. Burghard, K. Kern, U. Kaiser, *Nano Lett.* **2010**, 10, 1144.
- [15] H. Lee, K. Paeng, I. S. Kim, *Synth. Met.* **2018**, 244, 36.
- [16] H. Yamaguchi, S. Ogawa, D. Watanabe, H. Hozumi, Y. Gao, G. Eda, C. Mattevi, T. Fujita, A. Yoshigoe, S. Ishizuka, L. Adamska, T. Yamada, A. M. Dattelbaum, G. Gupta, S. K. Doorn, K. A. Velizhanin, Y. Teraoka, M. Chen, H. Htoon, M. Chhowalla, A. D. Mohite, Y. Takakuwa, *Phys. Status Solidi A* **2016**, 213, 2380.
- [17] H. K. Jeong, C. Yang, B. S. Kim, K.-j. Kim, *Europhys. Lett.* **2010**, 92, 37005.
- [18] A. Y. S. Eng, Z. Sofer, D. Sedmidubský, M. Pumera, *ACS Nano* **2017**, 11, 1789.
- [19] S. Javaid, M. J. Akhtar, E. M. Kim, G. Lee, *Surf. Sci.* **2019**, 686, 39.
- [20] Z. Luo, S. Lim, Z. Tian, J. Shang, L. Lai, B. MacDonald, C. Fu, Z. Shen, T. Yu, J. Lin, *J. Mater. Chem.* **2011**, 21, 8038.
- [21] M. Rybin, A. Pereyaslavtsev, T. Vasilieva, V. Myasnikov, I. Sokolov, A. Pavlova, E. Obraztsova, A. Khomich, V. Ralchenko, E. Obraztsova, *Carbon* **2016**, 96, 196.
- [22] Y. Jin, Y. Zheng, S. G. Podkolzin, W. Lee, *J. Mater. Chem. C* **2020**, 8, 4885.
- [23] C.-K. Chang, S. Kataria, C.-C. Kuo, A. Ganguly, B.-Y. Wang, J.-Y. Hwang, K.-J. Huang, W.-H. Yang, S.-B. Wang, C.-H. Chuang, M. Chen, C.-I. Huang, W.-F. Pong, K.-J. Song, S.-J. Chang, J.-H. Guo, Y. Tai, M. Tsujimoto, S. Isoda, C.-W. Chen, *ACS Nano* **2013**, 7, 1333.
- [24] M. Fan, Z.-Q. Feng, C. Zhu, X. Chen, C. Chen, J. Yang, D. Sun, *J. Mater. Sci.* **2016**, 51, 10323.
- [25] C.-S. Yang, Y. Han, Y. Ye, H. Pan, J.-O. Lee, J. Zhu, H. K. Jeong, *Chem. Phys. Lett.* **2013**, 559, 67.
- [26] D. S. Sutar, G. Singh, V. D. Botcha, *Appl. Phys. Lett.* **2012**, 101, 103103.
- [27] M. K. Rabchinskii, S. A. Ryzhkov, D. A. Kirilenko, N. V. Ulin, M. V. Baidakova, V. V. Shnitov, S. I. Pavlov, R. G. Chumakov, D. Y. Stolyarova, N. A. Besedina, A. V. Shvidchenko, D. V. Potorochin, F. Roth, D. A. Smirnov, M. V. Gudkov, M. Brzhezinskaya, O. I. Lebedev, V. P. Melnikov, P. N. Brunkov, *Sci. Rep.* **2020**, 10, 6902.
- [28] M. K. Rabchinskii, V. V. Shnitov, A. T. Dideikin, A. E. Aleksenskii, S. P. Vul', M. V. Baidakova, I. I. Pronin, D. A. Kirilenko, P. N. Brunkov, J. Weise, S. L. Molodtsov, *J. Phys. Chem. C* **2016**, 120, 28261.
- [29] M. K. Rabchinskii, A. S. Varezchnikov, V. V. Sysoev, M. A. Solomatina, S. A. Ryzhkov, M. V. Baidakova, D. Y. Stolyarova, V. V. Shnitov, S. I. Pavlov, D. A. Kirilenko, A. V. Shvidchenko, E. Y. Lobanova,

- M. V. Gudkov, D. A. Smirnov, V. A. Kislenko, S. V. Pavlov, S. A. Kislenko, N. S. Struchkov, I. I. Bobrinetskiy, A. V. Emelianov, P. Liang, Z. Liu, P. N. Brunkov, *Carbon* **2021**, 172, 236.
- [30] A. Ganguly, S. Sharma, P. Papakonstantinou, J. Hamilton, *J. Phys. Chem. C* **2011**, 115, 17009.
- [31] H. Darmstadt, C. Roy, *Carbon* **2003**, 41, 2662.
- [32] M. M. Brzhezinskaya, V. E. Muradyan, N. A. Vinogradov, A. B. Preobrajenski, W. Gudat, A. S. Vinogradov, *Phys. Rev. B* **2009**, 79, 155439.
- [33] M. K. Rabchinskii, S. D. Saveliev, D. Y. Stolyarova, M. Brzhezinskaya, D. A. Kirilenko, M. V. Baidakova, S. A. Ryzhkov, V. V. Shnitov, V. V. Sysoev, P. N. Brunkov, *Carbon* **2021**, 182, 593.
- [34] M. Brzhezinskaya, E. A. Belenkov, V. A. Greshnyakov, G. E. Yalovega, I. O. Bashkin, *J. Alloys Compd.* **2019**, 792, 713.
- [35] A. Dimiev, D. V. Kosynkin, L. B. Alemany, P. Chaguine, J. M. Tour, *J. Am. Chem. Soc.* **2012**, 134, 2815.
- [36] H. Yu, B. Zhang, C. Bulin, R. Li, R. Xing, *Sci. Rep.* **2016**, 6, 36143.
- [37] C.-H. Chuang, Y.-F. Wang, Y.-C. Shao, Y.-C. Yeh, D.-Y. Wang, C.-W. Chen, J. W. Chiou, S. C. Ray, W. F. Pong, L. Zhang, J. F. Zhu, J. H. Guo, *Sci. Rep.* **2014**, 4, 4525.
- [38] M. Aci, G. Lee, C. Mattevi, A. Pirkle, R. M. Wallace, M. Chhowalla, K. Cho, Y. Chabal, *J. Phys. Chem. C* **2011**, 115, 19761.
- [39] H. Cheng, Y. Huang, Q. Cheng, G. Shi, L. Jiang, L. Qu, *Adv. Funct. Mater.* **2017**, 27, 1703096.
- [40] M. Acik, G. Lee, C. Mattevi, M. Chhowalla, K. Cho, Y. J. Chabal, *Nat. Mater.* **2010**, 9, 840.
- [41] B. Gupta, N. Kumar, K. Panda, V. Kanan, S. Joshi, I. Visoly-Fisher, *Sci. Rep.* **2017**, 7, 45030.
- [42] V. Lee, R. V. Dennis, B. J. Schultz, C. Jaye, D. A. Fischer, S. Banerjee, *J. Phys. Chem. C* **2012**, 116, 20591.
- [43] D. A. Kirilenko, A. T. Dideykin, G. Van Tendeloo, *Phys. Rev. B* **2011**, 84, 235417.
- [44] R. Q. Zhang, E. Bertran, S.-T. Lee, *Diamond Relat. Mater.* **1998**, 7, 1663.
- [45] L. Rieppo, S. Saarakkala, T. Närhi, H. J. Helminen, J. S. Jurvelin, J. Rieppo, *Osteoarthritis Cartilage* **2012**, 20, 451.
- [46] A. Barrie, F. J. Street, *J. Electron Spectrosc. Relat. Phenom.* **1975**, 7, 1.
- [47] M. Favaro, G. A. Rizzi, S. Nappini, E. Magnano, F. Bondino, S. Agnoli, G. Granozzi, *Surf. Sci.* **2016**, 646, 132.
- [48] F. R. McFeely, S. P. Kowalczyk, L. Ley, R. G. Cavell, R. A. Pollak, D. A. Shirley, *Phys. Rev. B* **1974**, 9, 5268.
- [49] B. L. Henke, P. Lee, T. J. Tanaka, R. L. Shimabukuro, B. K. Fujikawa, *At. Data Nucl. Data Tables* **1982**, 27, 1.
- [50] W. von Niessen, *J. Electron Spectrosc. Relat. Phenom.* **1980**, 21, 175.
- [51] M. K. Orloff, N. B. Colthup, *J. Chem. Educ.* **1973**, 50, 400.
- [52] J. A. Pople, G. A. Segal, *J. Chem. Phys.* **1965**, 43, S136.
- [53] M. Bowker, R. J. Madix, *Surf. Sci.* **1981**, 102, 542.
- [54] S. Leacha, M. Schwella, D. Talbi, G. Berthierb, K. Hottmann, H.-W. Jochims, H. Baumgartel, *Chem. Phys.* **2003**, 286, 15.
- [55] G. Kresse, J. Furthmüller, *Phys. Rev. B* **1996**, 54, 11169.
- [56] R. S. Mulliken, *J. Chem. Phys.* **1955**, 23, 1841.
- [57] J. C. Woicik, E. J. Nelson, L. Kronik, M. Jain, J. R. Chelikowsky, D. Heskett, L. E. Berman, G. S. Herman, *Phys. Rev. Lett.* **2002**, 89, 077401.
- [58] M. K. Rabchinskii, V. V. Shnitov, D. Y. Stolyarova, S. A. Ryzhkov, M. V. Baidakova, E. Y. Lobanova, A. V. Shvidchenko, N. A. Besedina, D. A. Smirnov, *Fullerenes, Nanotubes, Carbon Nanostruct.* **2020**, 28, 221.
- [59] S. L. Molodtsov, S. I. Fedoseenko, D. V. Vyalikh, I. E. Iossifov, R. Follath, S. A. Gorovikov, M. M. Brzhezinskaya, Y. S. Dedkov, R. Püttner, J.-S. Schmidt, V. K. Adamchuk, W. Gudat, G. Kaindl, *Appl. Phys. A* **2009**, 94, 501.
- [60] J. Stöhr, *N. spectroscopy, Springer Series in Surface Sciences*, Springer-Verlag, New York, NY **1992**.
- [61] X. Zheng, B. Jia, H. Lin, L. Qiu, D. Li, M. Gu, *Nat. Commun.* **2015**, 6, 8433.
- [62] M. K. Rabchinskii, S. D. Saveliev, S. A. Ryzhkov, E. K. Nepomnyashchaya, S. I. Pavlov, M. V. Baidakova, P. N. Brunkov, *J. Phys.: Conf. Ser.* **2020**, 1695, 012070.
- [63] P. E. Blöchl, *Phys. Rev. B* **1994**, 50, 17953.
- [64] J. P. Perdew, K. Burke, M. Ernzerhof, *Phys. Rev. Lett.* **1996**, 77, 3865.
- [65] H. J. Monkhorst, J. D. Pack, *Phys. Rev. B* **1976**, 13, 5188.
- [66] G. Kresse, J. Furthmüller, *Comput. Mater. Sci.* **1996**, 6, 15.
- [67] I. Zacharov, R. Arslanov, M. Gunin, D. Stefonishin, A. Bykov, S. Pavlov, O. Panarin, A. Maliutin, S. Rykovanov, M. Fedorov, *Open Eng.* **2019**, 9, 512.